

Residues in the 11 Å Channel of Histone Deacetylase 1 Promote Catalytic Activity: Implications for Designing Isoform-Selective Histone Deacetylase Inhibitors[†]

Sujith V. W. Weerasinghe,[‡] Guillermina Estiu,[§] Olaf Wiest,[§] and Mary Kay H. Pflum^{*‡}

Department of Chemistry, Wayne State University, 5101 Cass Avenue, Detroit, Michigan 48202, and the Walther Cancer Research Center and Department of Chemistry and Biochemistry, University of Notre Dame, Notre Dame, Indiana 46556-5670

Received January 26, 2008

Histone deacetylase 1 (HDAC1) has been linked to cell growth and cell cycle regulation, which makes it a widely recognized target for anticancer drugs. Whereas variations of the metal-binding and capping groups of HDAC inhibitors have been studied extensively, the role of the linker region is less well known, despite the potency of inhibitors with diverse linkers, such as MS-275. To facilitate a drug design that targets HDAC1, we assessed the influence of residues in the 11 Å channel of the HDAC1 active site on activity by using an alanine scan. The mutation of eight channel residues to alanine resulted in a substantial reduction in deacetylase activity. Molecular dynamics simulations indicated that alanine mutation results in significant movement of the active-site channel, which suggests that channel residues promote HDAC1 activity by influencing substrate interactions. With little characterization of HDAC1 available, the combined experimental and computational results define the active-site residues of HDAC1 that are critical for substrate/inhibitor binding and provide important insight into drug design.

Introduction

Histone deacetylase (HDAC^a) proteins catalyze the removal of acetyl groups from acetylated lysines on histone substrates. The acetylation state of specific lysine residues in histone proteins can alter the chromatin structure and influence eukaryotic gene transcription.² Because of their fundamental role in gene expression, HDAC proteins are promising targets for cancer treatment, as shown by the recent FDA approval of the HDAC inhibitor suberoylanilide hydroxamic acid (SAHA, Vorinostat, Figure 1) for the treatment of cutaneous T-cell lymphoma. Additional HDAC inhibitors are currently in clinical trials to treat various cancers.^{3–5}

Anticancer HDAC inhibitors target 11 of the 18 known HDAC proteins. The inhibitor-sensitive proteins are divided into three classes on the basis of phylogenetic analysis.⁶ HDAC1, HDAC2, HDAC3, and HDAC8 are members of the class I subfamily and are homologous to yeast RPD3 protein.^{7–11} HDAC4, HDAC5, HDAC6, HDAC7, HDAC9, and HDAC10 belong to class II and are homologues to yeast HDA1 protein.^{12–14} HDAC11 is the only member of class IV in humans and is predicted to have diverged very early in evolution.^{6,15} Class I, II, and IV proteins display considerable sequence similarity in their catalytic sites, which suggests that they operate via similar metal-dependent deacetylase mechanisms.^{16,17} With conserved active sites, it is not surprising that many HDAC inhibitors nonspecifically influence the catalytic activity of the 11 HDAC proteins.

[†] This work was supported by the National Institutes of Health (GM067657) and Wayne State University.

* To whom correspondence should be addressed. Tel: (313) 577-1515. Fax: (313) 577-8822. E-mail: pflum@chem.wayne.edu.

[‡] Wayne State University.

[§] University of Notre Dame.

^a Abbreviations: HDAC, histone deacetylase; HDACi, HDAC inhibitor; RNAi, RNA interference; RbAp, Rb-associated protein; REST, RE1-silencing transcription factor/neural restrictive silencing factor; NuRD or NRD, nucleosome remodeling and deacetylating; SAP, Sin3A associated protein; MTA, metastasis-associated protein; MBD, Methyl-DNA binding domain; TSA, trichostatin; SDS-PAGE, sodium dodecyl sulfate polyacrylamide gel electrophoresis; IP, immunoprecipitation.

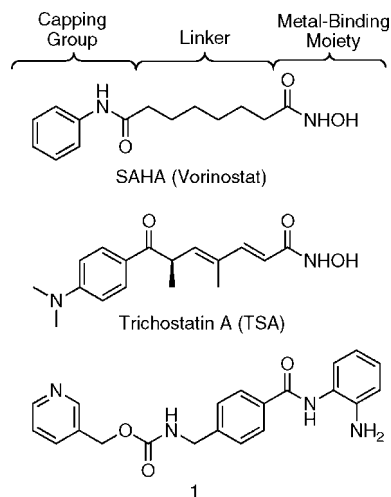


Figure 1. Structures of HDAC inhibitors SAHA, TSA, and MS-275 (1) with modular structures indicated.

Despite their role as anticancer targets, it is unclear which of the 11 HDAC proteins is involved in cancer formation. A candidate protein is HDAC1 because its activity has been linked to cellular proliferation, which is aberrant in cancer tissues. Specifically, an HDAC1 knockout in mice was embryonic lethal, and the resulting stem cells displayed altered cell growth and altered gene expression.^{18,19} Mammalian cells with RNA interference-mediated knockdown of HDAC1 expression were antiproliferative.²⁰ Finally, lengthened G2 and M phases and a reduced growth rate were observed in cells that overexpressed HDAC1.^{21,22} To explore the function of HDAC1 further, associated protein were identified by biochemical purification. HDAC1 exists in at least three distinct biochemical complexes: Sin3, NuRD (NRD), and CoREST.^{23–29} Interestingly, the NuRD complex contains metastasis-associated protein 2 (MTA2), which is linked to cancer metastasis, providing further evidence that HDAC1 plays a role in cancer development.^{30–32} Significantly, the coexpression of MTA2 and HDAC1 augmented the deacetylase activity,³³ which suggests that the presence of

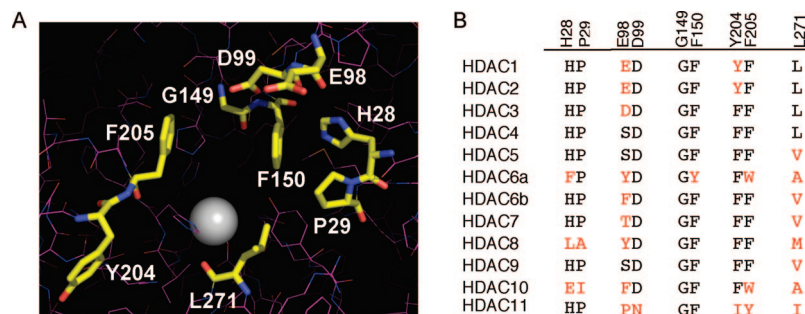


Figure 2. Residues in the substrate-binding channel of HDAC1. (A) The nine amino acids (ball–stick structures) lining the substrate-binding channel of the HDAC1 homology model are shown. The zinc, carbon, oxygen, and nitrogen atoms in the catalytic site are shown as gray, yellow, red, and blue balls, respectively. (B) We aligned catalytic domains of the class I, II, and IV human HDAC proteins by using Clustal W¹, and the residues located in the substrate-binding channel are shown. The residues that differ from the most highly conserved residue at each position are highlighted in red (Genbank Accession numbers: HDAC1-Q13547; HDAC2-Q92769; HDAC3-NP_003874.2; HDAC4-AAD29046.1; HDAC5-AAD29047.1; HDAC6-AAD29048.1; HDAC7-NP_056216.1; HDAC8-CAB90213.1; HDAC9-AAK66821.1; HDAC10-NP_114408.3; HDAC11-NP_079103.1).

associated proteins promotes the enzymatic activity of HDAC1. The combined data suggest that HDAC1 may be prominently involved in cancer formation because of its governing role in cell proliferation, which makes it a target for HDAC-inhibitor drug design.

Because of the likely role of HDAC1 in carcinogenesis, isoform-selective HDAC inhibitors that preferentially target HDAC1 would be important tools for exploring the role of HDAC1 in the regulation of gene expression and carcinogenesis. In addition, HDAC1-selective inhibitors may provide therapeutic advantages in chemotherapy.³⁴ Because of the widespread interest in HDAC inhibitors, extensive work has been performed by both industrial and academic researchers to discover novel HDAC inhibitors.³ Using the generally accepted pharmacophore model that divides the HDAC-inhibitor structure into a metal-binding moiety, a linker, and a capping group (Figure 1),³⁵ the majority of the inhibitor design so far has focused on the metal-binding and capping groups. In contrast, the role of the linker, which is generally analogous to the carbon chain in the lysine substrate, is less well understood. This is surprising because the X-ray structure of the HDAC-like bacterial homologue (HDLP) in complex with the HDAC inhibitor trichostatin (TSA, Figure 1) shows the interaction of a methyl group of the TSA linker with two Phe in the 11 Å channel (aligned with F150 and F205 in HDAC1).¹⁶ Furthermore, the experimentally observed potencies of MS-275 (**1**, Figure 1) and related HDAC inhibitors³⁶ show that structural variations in the linker moiety from straight chains to substituted arenes are possible. In addition, **1** demonstrates a modest selectivity for class I HDAC proteins,³⁶ which may result, in part, from the discrimination of the aromatic linker among the 11 Å channels of the HDAC isoforms. Because of the absence of structural information, the role of the 11 Å channel in substrate/inhibitor binding and its interaction with the linker group of inhibitors is unclear.

Structural insights into the substrate- or inhibitor-binding region of the active site would be useful in facilitating the design of HDAC1-selective inhibitors. Unfortunately, no structure of human HDAC1 has been reported. A homology model of human HDAC1 based on the crystal structure of HDLP has been proposed to aid in drug design.^{16,37–39} The model shows a high degree of structural similarity compared to the one crystallized human protein HDAC8;^{33,40} the amino acids involved in catalysis are located at the bottom of a roughly 11-Å-deep, narrow channel made up of seven

loops.^{37–39} The walls of the channel are covered with hydrophobic and aromatic residues (H28, P29, G149, F150, F205, and L271 in the HDAC1 sequence, Figure 2A) that likely interact with the substrate or the inhibitor. Interestingly, the phenyl groups of F150 and F205 (in HDAC1) face each other and are parallel to each other, forming the most slender portion (7.5 Å) of the channel. Because the channel exit is composed of loop regions, it has been hypothesized that this region is flexible.^{37–39} Consistent with this hypothesis, molecular dynamics (MD) simulations of the HDAC1 homology model in complex with the small-molecule inhibitor TSA (Figure 1) indicate a high degree of molecular motion near the entry point of the channel (F205 in HDAC1, for example). Density functional theory and QM/MM studies of the HDAC1 homologue HDLP indicate that channel residues H21 and E92 (H28 and D99 in HDAC1) stabilize the transition state of the deacetylase reaction through an extended hydrogen-bonding network despite their considerable distance from the catalytic site.¹⁷ Consistent with the hypothesis that channel residues promote HDAC function, the amino acids in the channel are well conserved among the class I, II, and IV human HDAC proteins (Figure 2B).⁴¹ The computational predictions suggest that some channel residues maintain considerable flexibility whereas others influence HDAC1 activity. Because residues in the channel interact with HDAC inhibitor drugs, particularly in the linker region, understanding the role of these residues in HDAC1 activity has the potential to aid in the design of selective inhibitors.^{37,39}

Mutagenesis studies were employed in probing the influence of residues in the 11 Å channel of HDAC1 on catalytic activity and associations. Specifically, an alanine scan of eight channel residues resulted in a 62–91% reduction in deacetylase activity, which revealed their importance in maintaining catalytic function. Because F150 and F205 were previously shown to create the narrowest region of the catalytic site, they were mutated to all other natural amino acids, which revealed that Phe at positions 150 and 205 is uniquely required for full catalytic activity. Finally, MD simulations indicate that the F150A mutation results in a disrupted substrate interaction surface, which was corroborated by a kinetics analysis. In total, the results suggest that the residues in the channel are critical in HDAC1 catalytic activity because they promote tight binding to the acetyllysine substrate. Significantly, the data identify specific residues in HDAC1 that create a unique inhibitor interaction surface, which

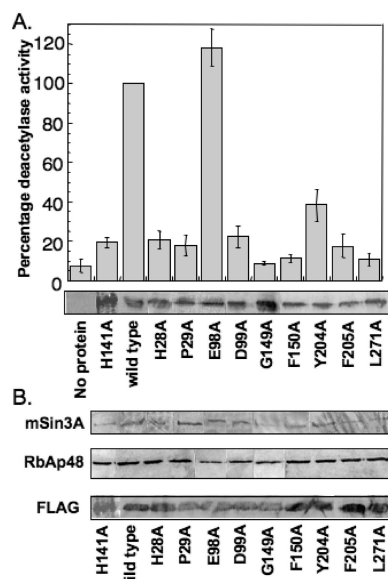


Figure 3. Channel residues of HDAC1 influence enzymatic activity but not protein association. (A) HDAC1 wild-type or alanine mutants were expressed as FLAG-tagged fusion proteins and were immunoprecipitated with anti-FLAG-agarose resin. The immunoprecipitated protein was used in fluorescence HDAC assays (histogram) in which the mean percent activity of five independent trials compared with that of the wild-type protein (100%) with standard error is shown. The immunoprecipitated proteins were also separated by SDS-PAGE and were probed with anti-FLAG (gel image) to ensure that equivalent protein quantities were used. We also confirmed the inactivity of F150A, F205A, and L271A by using a full-length hyperacetylated histone substrate (data not shown). (B) Immunoprecipitated proteins in part A were further probed with anti-mSin3A, anti-RbAp48, and anti-FLAG so that we could assess protein association.

provides the needed guidance for the future creation of HDAC1-selective inhibitors.

Results

Residues in the 11 Å Channel Are Critical for Deacetylase Activity. A homology model of HDAC1^{37–39} was used to identify nine amino acids that are likely to reside in the 11 Å channel of HDAC1: H28, P29, E98, D99, G149, F150, Y204, F205, and L271 (Figure 2A). These amino acids are not expected to promote catalysis directly because they reside near the solvent-exposed surface of the active-site channel. However, because of their proximity to the active site, the nine residues could potentially influence substrate binding and the orientation of the catalytic amino acids.

An alanine scan was used to determine the contribution to enzymatic activity of the nine residues that line the 11 Å channel. In particular, HDAC1 mutants were created in which each amino acid was individually mutated to alanine. In addition, a catalytically inactive H141A mutant was included for comparison.⁴² Wild-type and mutant proteins were expressed in Jurkat cells as FLAG-tagged fusion proteins, were immunoprecipitated with α -FLAG agarose, and were tested for catalytic activity by an *in vitro* fluorescence assay (Figure 3A). Channel residue mutants of HDAC1 significantly influenced HDAC catalytic activity (Table S1). In particular, the G149A, F150A, and L271A mutants demonstrated 8.7–11.3% activity compared with the wild type, which is comparable to the no-protein negative control (7.4%). Not surprisingly, these amino acids are highly conserved among the class I, II, and IV HDAC proteins (Figure 2B) and demonstrate 75% (L271) and 100% (G149 and F150) similarity. The homology model of HDAC1

predicts that G149, F150, and L271 are more buried in the 11 Å channel and are closer to the catalytic active site, which is consistent with their role in maintaining catalytic activity.^{37,39}

Mutations of several amino acids reduced the deacetylase activity to levels comparable to those of the H141A mutant (19.5%). In particular, the H28A, P29A, D99A, and F205A mutants displayed 17.6–20.5% activity compared with the wild type. Similar to G149, F150, and L271, these residues are also highly conserved among the human HDAC proteins, with percent similarities ranging from 75 (H28 and F205) to 91% (D99). In this case, the HDAC homology model predicts that H28, P29, D99, and F205 are positioned toward the solvent-exposed region of the 11 Å channel and are farther from the catalytic active site than G149, F150, and L271.^{37,39} Consistent with these findings, a mutation of D101 in HDAC8 (aligned with D99 in HDAC1) also resulted in a loss of enzymatic activity, which suggests structural similarities in the active sites of the HDAC isoforms.³³ The combined activity data suggest that H28, P29, D99, G149, F150, F205, and L271 promote the activity of HDAC1, and the data confirm the location of these residues in the HDAC1 active site.

The alanine mutations of two residues in the solvent-exposed region of the channel maintained significant levels of deacetylase activity. Compared with the wild type, Y204A demonstrated 38.2% activity. On the basis of the HDAC1 homology model,^{37,39} Y204 is expected to reside at the entrance of the 11 Å channel, which suggests that this solvent-exposed region of the protein can more flexibly accommodate mutation. In fact, among the class I, II, and IV HDAC proteins, position 204 is occupied by Phe in 75% of the families; only HDAC1 and HDAC2 contain a Tyr at that position. Only one mutant maintained deacetylase activity that was comparable to that of the wild type HDAC1. Specifically, E98A displayed 118% of wild-type activity. Not surprisingly, E98A is not well conserved across the class I, II, and IV HDAC proteins, and it shows only 25% sequence similarity. Like Y204, E98 is expected to sit at the entrance to the channel in the solvent-exposed region on the basis of the homology model of HDAC1.^{37,39} Therefore, among the residues in the 11 Å channel, only those likely to be most solvent-exposed can accommodate mutation. This conclusion is in agreement with observations from MD simulations that indicate a high degree of flexibility of the residues at the channel exit.^{37,39}

Mutation of Channel Residues Does Not Influence Protein Associations. HDAC1 interacts with various associated proteins and displays higher deacetylase activity when coexpressed with associated proteins,^{28,33} which suggests that protein associations and enzymatic activity are linked. Consistent with this observation, the mutation of several amino acids in the catalytic active site or the C-terminus of HDAC1 was previously shown to reduce protein associations and enzymatic activity.^{42,43} In contrast, the HDAC1 H141A mutant maintains interaction with RbAp48 and mSin3A proteins despite its reduced deacetylase activity.⁴²

The nine alanine mutants were immunoprecipitated as described, separated by SDS-PAGE, and probed with antibodies specific to mSin3A and RbAp48 so that we could determine the influence of channel residues on protein interactions. As shown in Figure 3B, the alanine mutants were capable of coimmunoprecipitating mSin3A and RbAp48. All mutants recovered similar amounts of RbAp48 after immunoprecipitation, independent of catalytic activity; HDAC1 mutants maintaining enzymatic activity (E98A and Y204A) displayed similar RbAp48 binding compared to inactive mutants (G149A, F150A, and L271A). As with RbAp48, all mutants also coimmunopre-

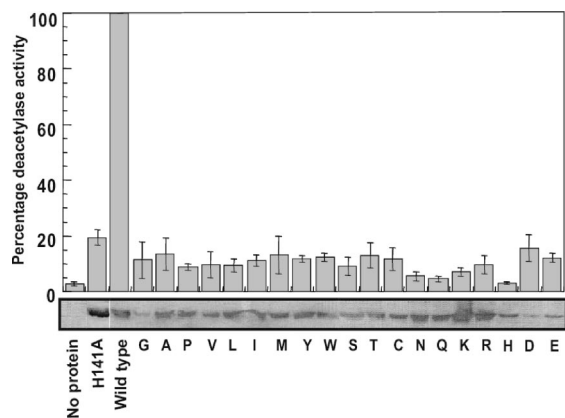


Figure 4. HDAC1 F150 uniquely promotes catalytic activity. HDAC1 wild type or mutants were expressed as FLAG-tagged fusion proteins and were immunoprecipitated with anti-FLAG-agarose resin. Immunoprecipitated proteins were used in fluorescence HDAC assays where the data represent the mean percent activity of three independent trials compared with that of the wild-type protein (100%). Standard error is shown. The immunoprecipitated proteins were also separated by SDS-PAGE and were probed with anti-FLAG (gel image) to ensure that equivalent protein quantities were used.

cipitated mSin3A. In this case, where the binding between the H141A mutant and mSin3A was slightly reduced compared to that of wild type HDAC1, H28A, G149A, and F205A also demonstrated modestly reduced association. The remaining mutants coimmunoprecipitated quantities of mSin3A that were comparable to those of the wild-type protein. The fact that all mutants were capable of coimmunoprecipitating RbAp48 and mSin3A reinforces the similarities with the H141A catalytic-site mutant. Significantly, the protein association data suggest that the global HDAC1 structure is not fundamentally disrupted upon channel-residue mutation.

F150 Is Strictly Required to Maintain HDAC1 Activity.

According to structural data of human HDAC8,^{33,40} the thermophilic bacterium homolog HDLP,¹⁶ and the HDAC1 homology model,^{37,39} two phenylalanine residues that reside in the 11 Å channel of HDAC1 (F150 and F205) make up the most slender region of the active site channel. In particular, the phenyl side chains of F150 and F205 face each other and are parallel to each other at a distance of 7.5 Å.¹⁶ When bound to the HDAC inhibitors TSA or SAHA (Figure 1), F150 and F205 sandwich the small molecules in their linker regions (Figure 1), which likely creates favorable hydrophobic contacts. Therefore, the structural data suggest that F150 and F205 are involved in the binding of the acetyllysine substrate via hydrophobic interactions. According to this hypothesis, a substitution of similar hydrophobic or aromatic side chains might maintain the catalytic activity of F150 and F205 mutants. To characterize the functional significance of F150 and F205 in HDAC1 more thoroughly, we first explored the catalytic activity of additional F150 mutants. F150 in HDAC1 was mutated into all other possible natural amino acids, and the resulting mutant proteins were expressed as FLAG-tagged fusion proteins, were immunoprecipitated, and were tested for deacetylase activity by an *in vitro* fluorescence assay (Figure 4). The substitution of F150 for any other amino acid significantly compromised the deacetylase activity (Table S2). In particular, the mutation of F150 to amino acids with a hydrophobic side chains (G, A, P, V, L, I, and M) resulted in activities similar to those of H141A, which indicates that hydrophobicity alone cannot account for the influence of F150 on catalytic activity. Moreover, the substitution of F150 for other aromatic amino acids (H, W, and Y)

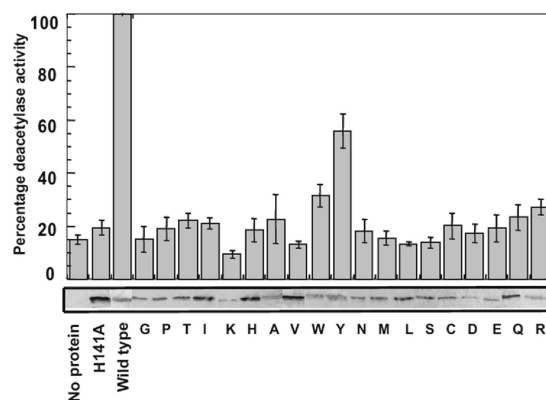


Figure 5. HDAC1 F205 activity is partially substituted by tyrosine. HDAC1 wild type or mutants were expressed as FLAG-tagged fusion proteins and were immunoprecipitated with anti-FLAG-agarose resin. Immunoprecipitated proteins were used in fluorescence HDAC assays where the data represent the mean percent activity of three independent trials compared with that of the wild-type protein (100%). Standard error is shown. The immunoprecipitated proteins were also separated by SDS-PAGE and were probed with anti-FLAG (gel image) to ensure that equivalent protein quantities were used.

also reduced the enzymatic activity, which indicates that aromatic interactions alone are not sufficient to maintain catalytic activity. Collectively, the data suggest that F150 is uniquely required in maintaining HDAC1 enzymatic activity via proper hydrophobic and aromatic interactions in the channel.

Tyrosine Partially Substitutes for F205. Because structural evidence suggests that F150 and F205 cooperate to form the tightest portion of the substrate-binding channel, the influence of F205 mutations on catalytic activity was also explored. As described for the F150 position, F205 in HDAC1 was mutated into all other natural amino acids, and the resulting mutant proteins were expressed as FLAG-tagged fusion proteins, were immunoprecipitated, and were tested for deacetylase activity (Figure 5). Similar to the F150 mutational analysis, the substitution of F205 with acidic, basic, or hydrophobic amino acids resulted in enzymatic activity comparable to that of the H141A mutant (Table S3). In this case, however, three mutants displayed catalytic activity that was statistically greater than that of the H141A mutant. The F205Y mutant showed 56% activity compared to the wild type. Because Tyr is structurally most similar to Phe among the natural amino acids, this is the most conservative possible mutation. The presence of phenolic alcohol, however, results in a significant reduction in catalytic activity compared to the wild type. The F205W mutant also demonstrated 31% of the wild-type activity. In this case, the indole side chain of Trp may partially substitute for Phe as a result of its aromatic character. In contrast, the F205H mutant demonstrated activity that was comparable to H141A despite its aromatic character. As in the F150 series, the presence of an aromatic side chain alone at position 205 is not sufficient to maintain catalytic activity. Surprisingly, the F205R mutant maintained 27% of the wild-type activity, which is slightly greater than the activity of H141A (19%).

F150/F205 Double Mutants Are Inactive. Because the phenyl side chains of F150 and F205 face each other and are parallel to each other at a distance of 7.5 Å and because they sandwich small-molecule inhibitors,¹⁶ they likely collaborate to promote HDAC1 catalytic activity. A single mutation in either F150 or F205 may disrupt the optimal substrate-binding surface, which results in the observed inactivity. Therefore, we wondered if a mutation of both F150 and F205 to structurally compli-

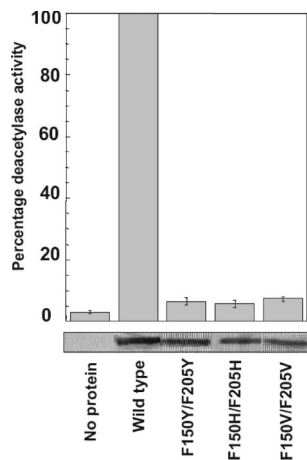


Figure 6. F150 and F205 double mutants are inactive. HDAC1 wild type or mutants were expressed as FLAG-tagged fusion proteins and were immunoprecipitated with anti-FLAG-agarose resin. Immunoprecipitated proteins were used in fluorescence HDAC assays where the data represent the mean percent activity of three independent trials compared with that of the wild-type protein (100%). Standard error is shown. The immunoprecipitated proteins were also separated by SDS-PAGE and were probed with anti-FLAG (gel image) to ensure that equivalent protein quantities were used.

mentary residues would mimic the natural substrate interaction surface to restore activity. For example, the substitution of F150 and F205 for complimentary hydrophobic (V) or aromatic residues (Y or H) might provide a substrate-binding surface that promotes activity. To explore the existence of compensating interactions by F150 and F205, we created the F150V–F205V, F150Y–F205Y, and F150H–F205H double mutants, and the resulting mutant proteins were expressed as FLAG-tagged fusion proteins, were immunoprecipitated, and were tested for deacetylase activity (Figure 6). Even though F205Y showed 56% activity compared with the wild type (Figure 5), the F150Y–F205Y double mutant displayed activity that was comparable to that of the negative control (Table S4). Similarly, the substitution with aromatic residue His (F150H–F205H) also resulted in inactivity. Consistent with the single-point mutants, the presence of aromatic side chains is not sufficient to promote activity. In addition, double substitution with the hydrophobic residue Val did not promote activity. In total, the data are consistent with the unique requirement for Phe at positions 150 and 205, which create the narrowest regions of the 11 Å channel of HDAC1.

Computational Analysis of Alanine Mutants Reveals a Disrupted Substrate Interaction Surface. The mutagenesis data suggest that residues in the 11 Å channel contribute to the HDAC1 catalytic function and, in the case of F150 and F205, the conserved residues uniquely promote catalytic activity. The structural origin of these observations is less clear. To gain insight into the structural role of channel residues in promoting HDAC1 activity, we computationally studied several mutant HDAC1 proteins. Simple models of the in silico mutated structures were generated by energy minimization, and the effect of the mutation was analyzed through a comparison to the similarly minimized structure of the wild-type HDAC1 homology model.^{37,39} No significant changes were noticeable after minimization for H28A, P29A, D99A, G149A, F205A, and L271A. In the case of the F150A mutant, however, the absence of the phenyl side chain in the wall of the 11 Å channel allows neighboring residues to move toward the previously occupied position. The movement of the thioether side chain of M30 toward F205 is the most noticeable effect in this stage of the computations (Figure 7A). A concomitant shift of the phenyl

side chain of F205 can also be inferred from Figure 7A. However, geometry optimization does not properly sample the conformational space, and protein reorganization must be analyzed by the use of a dynamic approach that evaluates positions averaged over time. Therefore, definitive conclusions cannot be derived from the analysis of the minimized structures. Rather, these structures are the basis for the selection of promising mutations for further MD studies.

Following the results of the geometry optimizations, the F150A mutant and the wild-type HDAC1 model were analyzed during 2 ns MD simulations. The structures are sufficiently equilibrated and stable under NTP conditions (see rmsd plots, Figure S1) with no change in the geometry of the catalytic active site in either the mutant or the wild-type structure (Figure S2).

The role of F150 and F205 in the catalytic activity of HDAC proteins has been largely discussed in relation to substrate binding.^{16,40,44} X-ray determinations show that the side chains of the residues are assembled in a parallel orientation, which leads us to assign a special role to these residues in establishing π – π stacking interactions with inhibitors.^{16,40} Recent studies have compared the activities of inhibitors bearing aromatic or aliphatic portions that are in a position that is suitable to accommodate between F150 and F205.⁴⁴ The similar activities of aromatic and aliphatic structures as well as the relatively large distance between the rings suggested that hydrophobic interactions of ligands with either one or both residues occurred rather than π -stacking interactions. Molecular dynamics simulations of the wild-type enzyme without a bound ligand show that both residues flip during the 2 ns simulation and adopt different orientations relative to each other (Figure 7B). This flipping is more significant for F205 probably because of its closeness to the channel entrance. As a way of quantifying this effect, we have plotted the dihedral angle that is defined by the phenyl rings of F150 and F205 (measured as F150C β –F150C γ –F205CE2, Figure 7C). The angle varies between 0 and 150°, with a mean value of 7°. The preference for the parallel orientation is in agreement with what is observed in the X-ray structure^{16,40,44} but is a result of time averaging. Thus it is of interest to analyze the relative importance of both residues in inhibitor binding.

The evolution of the F150A mutant during the 2 ns MD simulation provides more reliable conclusions on the cooperative interactions of both residues. The mutation triggers a significant movement of the loop that contains F205, whose flexibility appears to be constrained in the wild-type enzyme through cooperative interactions with F150 (Figure 7D). The loop opens away from the channel, which causes a distortion that is large enough, after a 2 ns MD run, to impair substrate binding (Figure 7E). The movement can be quantified by the distance between F205 and A150, which increases almost 10 Å, measured from C β of F205 to C α of A150 (Figure 7D). The F150A mutation also adds flexibility to the loop that contains M30, which supports the preliminary observation that was based on the analysis of the minimized structures. It is interesting to note that this loop is involved in the definition of the 14 Å internal cavity (see Figure 7F), which has been hypothesized to help the catalytic pathway by promoting the release of the acetate byproduct.³⁸ Thus the data are consistent with the hypothesis that the F150A mutation leads to an altered channel shape resulting in a disrupted binding to the acetyllysine substrate and a loss of catalytic activity. Similar results were found in 2 ns MD simulations of G149A and L271A, both of which resulted in a movement of F150, which will lead to a similar loss of hydrophobic interactions with the linker region, as described above (Figure S7 and S8).

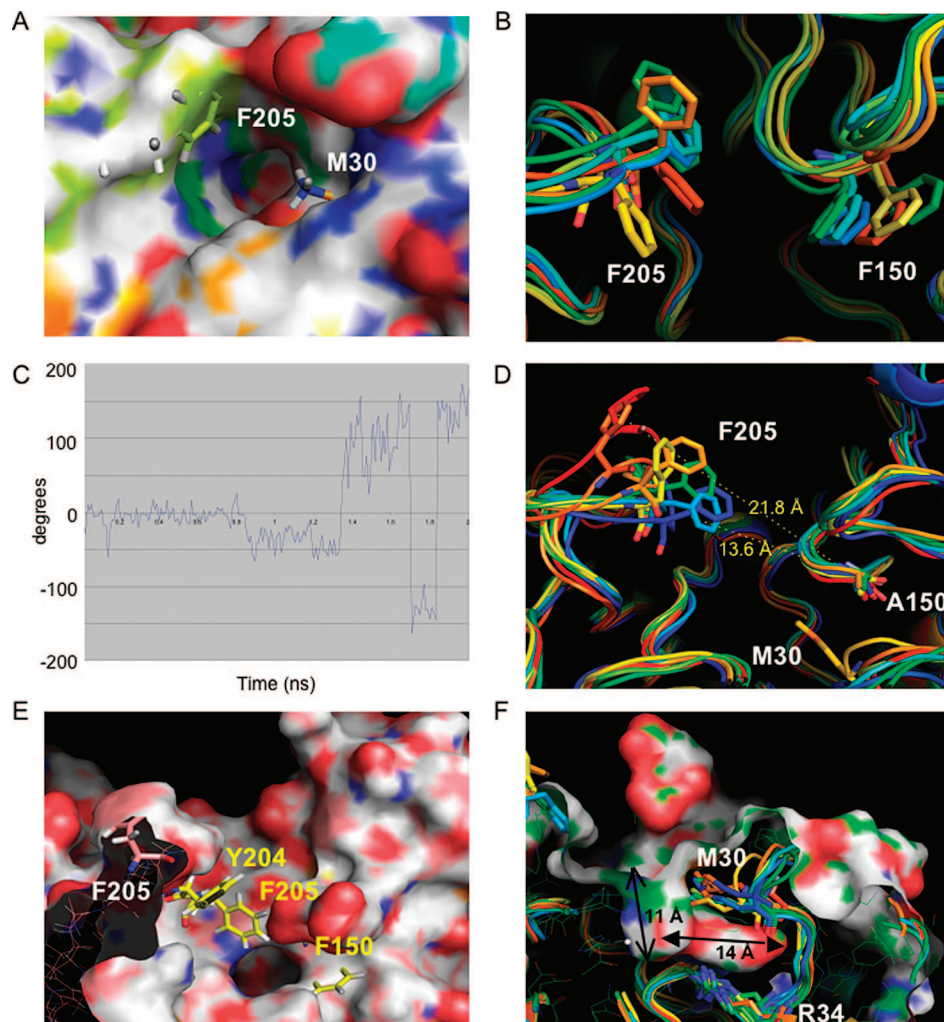


Figure 7. Molecular modeling and 2 ns dynamics simulations of the wild-type and the F150A mutant protein before optimization. (A) Surface representation of the F150A mutant protein before optimization. The structure is superimposed with the stick representation of the optimized structure, which shows the shifting of M30 toward the 11 Å channel. (B) Superposition of six snapshots (different colors) from the 2 ns MD runs of the wild-type homology model showing the flipping of F150 and F205 over time. (C) Dihedral angle defined by $F150\beta150C\gamma-F205C\gamma-F205CE2$ as a function of time. (D) Superposition of six snapshots (different colors) taken from the 2 ns MD runs of the F150A mutant showing the increased flexibility of the F205-containing loop. The distances between the residues (shown in yellow) are measured from A150C α to F205C γ for the first snapshot (blue) and the last snapshot (red). (E) Superposition of the last snapshot of the wild-type and the F150A mutant after 2 ns of MD simulation. A surface representation is displayed for the F150A structure to help locate the 11 Å channel. The stick representation is shown in red for F150A and in yellow for the wild-type structure. (F) Surface representation of the 11 Å channel and the 14 Å internal cavity of F150A. The loop containing M30 and the stick representations of M30 and R34 are shown for several snapshots.

Kinetics Analysis of HDAC1 F150A. The computational analysis predicts that the F150A mutation leads to altered substrate binding, which results in a loss of enzymatic activity. To test the computational analysis experimentally, we performed steady-state kinetics measurements with the HDAC1 wild-type and F150A mutant proteins. We rationalized that the K_m values of the F150A mutant and wild-type proteins would be significantly different if the F150A mutant displayed reduced substrate binding compared with the wild-type protein. Immunoprecipitated HDAC1 from Jurkat cells was used for the kinetics analysis, as previously reported,⁴⁵ because recombinant HDAC1 is inactive when it is expressed in bacteria or yeast.⁴⁶ Whereas immunoprecipitated HDAC1 exists in multiple complexes *in vivo*, the wild-type and F150A mutant proteins associate with similar complexes (Figures 3B and S5), which allows us to compare their activities.

We tested immunoprecipitated wild-type and F150A mutant proteins by using the *in vitro* fluorescence assay with varying concentrations of substrate over time, and the K_m values were

calculated. Wild-type HDAC1 displayed a K_m value of 88 μM , which is similar to previous kinetics measurements that used a different peptide substrate.^{45,47} The F150A mutant displayed a K_m value of 66 μM , which indicates that the mutant binds slightly better to the substrate than the wild-type protein does (Table 1). The kinetics data are not consistent with the computational prediction that the F150A mutant demonstrates reduced enzymatic activity as a result of a loss of substrate binding.

In contrast with the K_m values, the F150A mutant demonstrated a significantly reduced V_{max} value compared with that of the wild-type protein. Therefore, the primary effect on the F150A mutant activity is a significantly slower rate, with a V_{max} value that is roughly 12 times lower than that of the wild-type protein (Table 1). The kinetics assessment is consistent with earlier data that indicate that the F150A mutant displays only 11% of the wild-type activity (Figures 3A and S3). In total, the kinetics data indicate that the loss of the deacetylase efficiency

Table 1. Kinetics Study of the HDAC1 Wild Type and F150A Mutant^a

HDAC1	V_{\max} ($\mu\text{M/s}$)	K_m (μM)
wild type	6.5 ± 0.6	88 ± 3
F150A	0.52 ± 0.03	66 ± 2

^a Calculated from at least three independent trials with standard error shown. Protein expression was confirmed by Western blot (data not shown).

of the F150A mutant is primarily due to the slower rate of reaction not reduced substrate binding.

Discussion

Residues in the 11 Å channel are well conserved among the class I, II, and IV human HDAC proteins (Figure 2B), which suggests that they may play a role in HDAC function. Molecular dynamics simulations with the HDAC1 homology model indicate some flexibility in the amino acids that comprise the channel.^{37,39} In addition, the docking of small molecules in the HDAC active site suggests that the differences in the channel residues might play a role in inhibitor binding affinities,³⁸ which can aid the design of isoform-selective HDAC inhibitors. Unfortunately, no structural analysis of HDAC1 has been reported to confirm the computational analysis.

To investigate the influence of residues on HDAC1 substrate binding and activity, we explored the channel residues leading to the active site of HDAC1 by alanine scan mutagenesis.⁴⁸ Alanine was a poor substitute for H28, P29, D99, G149, F150, Y204, F205, and L271, which resulted in a 62–91% reduction in enzymatic activity compared with that of the wild-type protein. Because F150 and F205 create the narrowest portion of the 11 Å channel, these two positions were explored more thoroughly by mutagenesis. Phenylalanine was uniquely suited to promote HDAC1 catalytic activity at both positions, which indicates that these amino acids are critical in promoting HDAC1 activity. Only one mutant, F205Y, maintained significant enzymatic activity (56% compared with that of the wild-type HDAC1). The unique requirement of F150 is also consistent with kinetics studies, which showed that the F150A mutant displayed a reduced V_{\max} compared with the wild-type protein. The negative influence of channel residue mutations on catalytic activity indicates that the structure of the 11 Å channel is integral to the formation of an active HDAC1 protein.

Understanding the structure and function of HDAC1 will facilitate a characterization of HDAC1-mediated cancer formation and guidance for drug-design efforts. Unfortunately, a structural characterization of HDAC1 has been challenging because recombinant HDAC1 from bacteria is inactive, and mammalian cell-expressed HDAC1 is contaminated with associated proteins.⁴⁶ As an alternative, the mutagenesis studies presented here provide valuable insight into a structural characterization of HDAC1. Specifically, the data confirm the HDAC1 homology model's prediction that H28, P29, D99, G149, F150, Y204, F205, and L271 reside in the 11 Å channel.^{37,39} Combined with the previous mutagenesis,⁴² the results establish the identity of residues comprising the HDAC1 active site and channel regions.

One hypothesis that accounts for the influence of the 11 Å channel residue on HDAC1 activity is that mutagenesis reorganizes active-site amino acids, which leads to diminished activity. This hypothesis is supported by previous QM/MM studies that suggest that two channel residues (H28 and D99 of HDAC1) stabilize the transition state of the reaction despite their distance from the active site.¹⁷ To probe this hypothesis, we performed molecular modeling and dynamics simulations to assess the influence of channel residues on the structure of

the catalytic active site. The distances between the catalytic Zn^{2+} and nearby H178, D176, and D264 were similar in the F150A mutant as compared with wild-type HDAC1 (Figure S2). In addition, no change in the distances was observed over the 2 ns simulation in either the mutant or the wild-type structure (Figure S2). The dynamics simulation suggests that the tight hydrogen-bonding network that is expected in the HDAC1 active site on the basis of the homology model is resilient to small structural changes in the relatively distant 11 Å channel. Consistent with the computation, the channel residue mutants maintained an interaction with associated proteins (Figure 2B), which suggests that their global protein structures are not significantly altered. The combined computational and experimental evidence suggests that the channel-residue mutants maintain a properly structured catalytic site despite the loss of enzymatic activity.

A second possibility is that channel residues govern the substrate binding, which can influence the HDAC1 enzymatic activity. This hypothesis is consistent with crystallographic evidence that shows that residues in the 11 Å channel surround bound small-molecule inhibitors, which likely contributes to their binding affinities.^{37,39} To probe the influence of residues in the channel on HDAC1 structure and ligand binding, we performed MD simulations. First, the motion in the channel residues was determined with the wild-type protein. Wild-type HDAC1 showed a significant flexibility in the channel residues, particularly at the Y204 and F205 positions. Interestingly, the phenyl ring at the F205 position rotated around the C1–C4 axis of the phenyl ring during the 2 ns dynamics simulation. In the static-picture X-ray structures and the HDAC1 structural model based on them,^{16,33,37,39,40} the phenyl rings of F150 and F205 are found to be parallel and roughly 7.5 Å apart. Therefore, this arrangement is most likely due to a time averaging in the structure rather than a long-range interaction between the phenyl rings. Whereas Y204 and F205 displayed significant rotations prior to ligand binding, this rotation is limited upon the binding of an inhibitor in the channel, as was previously shown.^{37,39}

The molecular modeling and dynamics simulations were then analyzed for the F150A mutant. Similar to that observed in the wild-type protein, significant flexibility was observed in the channel residues of the F150A mutant, particularly at Y204 and F205 positions. In this case, the F205 position showed significantly greater motion compared with the Y204 position and oriented the phenyl side chain away from the channel. Because the wild-type structure suggests an interaction between the phenyl groups of F150 and F205, it is possible that the loss of this interaction in the F150A mutant results in more flexible movements of F205 away from the channel. Combined with the fact that the thioether side chain of the M30 residue only partially occupies the space that was left empty by the loss of F150, the data suggest a relative enlargement of the 11 Å channel at its narrowest point. Interestingly, a similar result is obtained from a 2 ns simulation of the F150Y mutant. Although Phe and Tyr are structurally similar, the F150Y mutant was also inactive (Figure 4). The MD simulation (Figure S6) reveals that the hydroxyl group of the tyrosine in the F150Y mutant participates in a hydrogen bond with D99, which opens up the channel for F205 to undergo a flip that is very similar to the one observed in the MD simulations of the F150A mutant (Figure 7D). Because residues in the 11 Å channel are expected to surround the substrate when they are bound,^{37,39} the widening of the channel upon mutation likely influences substrate binding by removing critical contacts with an inhibitor or a substrate. The computational results are consistent with the observation

that Phe is uniquely required at position 150 for enzymatic activity (Figure 4) by suggesting that the phenyl side chain creates an ideal substrate-binding surface.

To test the possibility that a loss of catalytic activity by the F150A mutant is due to perturbed substrate binding, we performed a kinetics assessment. Because the kinetic studies indicate similar K_m values for the F150A mutant and wild-type HDAC1 (Table 1), the predominant dictator of F150A activity is the reaction rate; the V_{max} value for the F150A mutant is roughly 12 times less than that of the wild type. We conclude from the kinetics analysis that the F150A mutant demonstrates a decreased deacetylase activity that is primarily due to a relative slowing of the reaction rate and not to reduced substrate binding. V_{max} mutants that display reduced activity as a result of a decreased reaction rate are well characterized.^{49,50} In these cases, changes in the transition-state complex account for an altered V_{max} without a necessary influence on K_m . Therefore, the kinetics data suggest that the loss of F150A mutant activity is a result of altered substrate binding in the tight active site that perturbs the transition-state complex and the rate of reaction. Consistent with this model, the computational analysis indicates that the active-site channel of the F150A mutant is relatively enlarged and likely perturbs the tight binding of the substrate. In addition, previous QM/MM studies showed that some of the channel residues stabilize the transition state of the reaction despite their distance from the active site.¹⁷ Finally, the mutation of D101 of HDAC8 (aligned with D99 in HDAC1) resulted in a loss of enzymatic activity that was likely due to an altered substrate interaction surface,³³ which suggests that active-site residues sustain a similar role in other HDAC isoforms. In total, the experimental and computational analyses suggest that the residues in the 11 Å channel are responsible for the proper positioning of the substrate in the active site, which is necessary in maintaining enzymatic activity.

By establishing the importance of channel residues in HDAC1 catalytic activity and substrate binding, the computational and mutagenesis results have implications for the development of new chemical tools. HDAC1 is a likely target for anticancer drugs, which makes the isolation of inhibitors with selectivity toward HDAC1 a valuable tool in the characterization of HDAC1-mediated cancer. The mutagenesis results reinforce the conclusion of previous computational studies that suggests that amino acid differences in the channel residues could be exploited to create isoform-selective HDAC inhibitors.^{37,39} In particular, the incompatibility of Ala in the P29 and L271 positions of HDAC1, despite its presence in other HDAC isoforms (Figure 2B), implies that this region of the HDAC1 active site is distinct from the other HDAC proteins. Several HDAC family members display either Tyr or Trp at the corresponding F150 and F205 positions in HDAC1 (Figure 2B). Because Tyr or Trp did not mimic F150 or F205 in the HDAC1 active site, these data provide further evidence of distinct channel regions among the HDAC isoforms. Importantly, the fact that the F150A mutant displays a similar K_m compared to the wild type suggests that residues in the 11 Å channel maintain flexibility and can accommodate bulky inhibitors. Therefore, the mutagenesis results raise the possibility of developing selective HDAC1 inhibitors by targeting structural differences at the P29, F150, F205, and L271 positions.

An interesting result of the mutagenesis is the fact that the E98A mutant maintained 118% deacetylase activity, a slight increase compared with that of the wild type (Figure 3A). Consistent with this observation, the E98 position lacks clear conservation among the HDAC family members (Figure 2B).

Previous alanine scanning experiments with human growth hormone (hGH) identified one residue (E174) that, when mutated, enhanced binding to the hGH receptor, which suggests that it acts as a gatekeeper to hinder ligand binding naturally.⁴⁸ In the case of kinases, the mutation of I338 in the substrate-binding region of v-Src kinase highlighted its role as a molecular gate for substrate interactions.⁵¹ On the basis of these previous studies, it is interesting to speculate that the E98 position represents a molecular gate that has the potential to impact inhibitor binding. In this scenario, the identity of the corresponding E98 position in the other HDAC proteins could be exploited to develop isoform-selective HDAC inhibitors. Specifically, charged or bulky groups at the corresponding E98 position in HDAC family members would suggest the creation of inhibitors with electronically or sterically compatible moieties. Therefore, a significant outcome of the combined experimental and computational data is the conclusion that differences in the charge and the shape of the 11 Å channel should be exploited in the creation of isoform-selective HDAC inhibitors.

Because the homology model of HDAC1 in complex with small-molecule inhibitors indicates that the linker region is positioned near residues in the 11 Å channel,^{37,39} the results suggest that a modification of the linker region may impart isoform-selectivity. In fact, small molecules with aryl groups in their linker regions, such as **1**, display modest isoform selectivity.³⁶ Therefore, the results encourage additional characterization of the role of the linker region of HDAC inhibitors in isoform selectivity.

Experimental Procedures

Mammalian Expression and Immunoblotting of HDAC1 Mutants. We cloned HDAC1 mutants into pBJ5HDAC1-F⁴³ by using the *NotI* and *EcoRI* sites (see Supporting Information for primer sequences), and all mutagenesis was confirmed by DNA sequencing. T-Ag Jurkat cells⁵² were grown in RPMI-1640 that was supplemented with 10% FBS and 1% antibiotic-antimycotic solution (GIBCO). pBJ5HDAC1-F or mutant expression plasmids (20 µg) were independently transiently transfected by electroporation into 40×10^6 T-Ag Jurkat cells. Cells were harvested 48 h post-transfection and were stored at -80°C until the analysis. Cells were lysed by incubation with JLB buffer (Tris, pH 8; 150 mM NaCl; 10% glycerol; 0.5% Triton X-100) that was supplemented with 1× protease inhibitor cocktail set V (Calbiochem). Expressed wild-type and mutant FLAG-tagged HDAC1 proteins were immunoprecipitated from the lysates by the use of 10 µL of anti-FLAG agarose beads (Sigma), were separated by 8% SDS-PAGE, and were transferred to PVDF membrane (Immobilon). The membrane was probed with the appropriate antibody: anti-FLAG (Sigma), anti-RbAp48 (Upstate), or anti-mSin3A (Santa Cruz).

HDAC Activity Assay and Kinetics. A Fluor de Lys fluorescence activity assay (Biomol) was used to measure the activity of wild-type and mutant HDAC1 proteins. In brief, wild-type or mutant proteins from roughly 20×10^6 cells were immunoprecipitated as described above (25 µL) and were incubated with 100 µM substrate (25 µL) at 37°C for 45 min with shaking (900 rpm), followed by the addition of developer (50 µL). After 5 min of shaking (500 rpm), the fluorescence signal was measured by the use of a GENios plus plate-reading fluorimeter (Tecan). The fluorescence signal for each mutant was normalized to that of the wild-type protein, and the standard error of at least three independent experiments is shown.

To perform the kinetics assessment, we incubated immunoprecipitated wild-type protein from roughly 3×10^6 cells per reaction (25 µL) with 50–600 µM of Fluor de Lys substrate, as described above, for between 4 and 16 min (Figure S3). In the case of the F150A mutant, 50–1000 µM substrate was incubated, as described above, for between 15 and 60 min. In each case, we converted fluorescence units (FU) to µM concentration by using the experi-

mentally determined fluorescence of the deacetylated substrate product (15.0 FU/ μ M). In addition, we normalized the FU signal in each trial for protein expression by using Western blot analyses. The data were fit to a Michaelis–Menten curve to determine V_{\max} and K_m (Figure S4).

Molecular Modeling and Dynamics Simulations. The homology model of HDAC1 that was previously developed by some of us^{37–39} has been used to model and analyze the effect of the mutations. H28A, P29A, D99A, G149A, F150A, F205A, and Y271A point mutations were generated by the use of PyMOL.⁵³ The resulting structures as well as the wild-type HDAC1 model were studied using AMBER 8.⁵⁴

The LEaP module of AMBER 8 was used to assign the protonation states and to maintain the overall neutrality of the system. The nonbonded model was used for the Zn^{2+} atom,⁵⁵ and standard AMBER02 force-field parameters were assigned to the HDAC proteins. The systems were then surrounded by a periodic box of TIP3P water molecules, which extends approximately 10 Å from the protein surface. Conjugate-gradient energy minimization was used to remove unfavorable contacts from the initial geometries and to stabilize the systems after the mutations (2500 steps for the water molecules, followed by 15 000 steps for the entire system). On the basis of the analysis of the mutated structures, the F149A, F150A and L271A mutants were selected for further analysis.

For the HDAC1 model and for the F150A, F150Y, G149A, and L271A structures, 2 ns MD simulations were carried out using the SANDER module of AMBER 8. We controlled the pressure (1 atm) and the temperature (300 K) of the system during the MD simulations by utilizing Berendsen's algorithms.⁵⁶ Periodic boundary conditions were applied to simulate a continuous system. Long-range interactions were treated by the particle-mesh Ewald (PME)⁵⁷ method. A time step of 1.0 fs was used to integrate the equations of motion, and the Shake⁵⁸ algorithm was used to constrain all bonds that involved hydrogen atoms. A nonbonded pair-list cutoff of 9.0 Å was used and was updated every 25 time steps. We analyzed all MD results by using the Ptraj module of AMBER 8⁵⁴ and visualized them by using PyMOL.⁵³

Acknowledgment. We thank the National Institutes of Health (GM067657) and Wayne State University for funding, the Walther Cancer Research Center at the University of Notre Dame for continuing support, S. L. Schreiber for the HDAC1 expression construct, and E. Aubie, F. Bittencourt, A. Feig, and P. Karwowska-Desaulniers for comments.

Supporting Information Available: Mutagenesis procedure and primer sequences, deacetylation assay and kinetics measurements, and computational data. This material is available free of charge via the Internet at <http://pubs.acs.org>.

References

- Chenna, R.; Sugawara, H.; Koike, T.; Lopez, R.; Gibson, T. J.; Higgins, D. G.; Thompson, J. D. Multiple sequence alignment with the Clustal series of programs. *Nucleic Acids Res.* **2003**, *31*, 3497–500.
- Grunstein, M. Histone acetylation in chromatin structure and transcription. *Nature* **1997**, *389*, 349–352.
- Dokmanovic, M.; Clarke, C.; Marks, P. A. Histone deacetylase inhibitors: overview and perspectives. *Mol. Cancer Res.* **2007**, *5*, 981–989.
- Ryan, Q. C.; Headlee, D.; Acharya, M.; Sparreboom, A.; Trepel, J. B.; Ye, J.; Figg, W. D.; Hwang, K.; Chung, E. J.; Murgo, A.; Melillo, G.; Elsayed, Y.; Monga, M.; Kalnitskiy, M.; Zwiebel, J.; Sausville, E. A. Phase I and pharmacokinetic study of MS-275, a histone deacetylase inhibitor, in patients with advanced and refractory solid tumors or lymphoma. *J. Clin. Oncol.* **2005**, *23*, 3912–3922.
- Kelly, W. K.; O'Connor, O. A.; Krug, L. M.; Chiao, J. H.; Heaney, M.; Curley, T.; MacGregore-Cortelli, B.; Tong, W.; Secrist, J. P.; Schwartz, L.; Richardson, S.; Chu, E.; Olgac, S.; Marks, P. A.; Scher, H.; Richon, V. M. Phase I study of an oral histone deacetylase inhibitor, suberoylanilide hydroxamic acid, in patients with advanced cancer. *J. Clin. Oncol.* **2005**, *23*, 3923–3931.
- Gregoret, I.; Lee, Y.-M.; Goodson, H. V. Molecular evolution of the histone deacetylase family: functional implications of phylogenetic analysis. *J. Mol. Biol.* **2004**, *338*, 17.
- Taunton, J.; Hassig, C. A.; Schreiber, S. L. A mammalian histone deacetylase related to the yeast transcriptional regulator Rpd3p. *Science* **1996**, *272*, 408–411.
- Yang, W.-M.; Inouye, C.; Zeng, Y.; Bearss, D.; Seto, E. Transcriptional repression by YY1 is mediated by interaction with a mammalian homolog of the yeast global regulator RPD3. *Proc. Natl. Acad. Sci. U.S.A.* **1996**, *93*, 12845–12850.
- Yang, W. M.; Yao, Y. L.; Sun, J. M.; Davie, J. R.; Seto, E. Isolation and characterization of cDNAs corresponding to an additional member of the human histone deacetylase gene family. *J. Biol. Chem.* **1997**, *272*, 28001–28007.
- Hu, E.; Chen, Z.; Fredrickson, T.; Zhu, Y.; Kirkpatrick, R.; Zhang, G.-F.; Johanson, K.; Sung, C.-M.; Liu, R.; Winkler, J. Cloning and characterization of a novel class I histone deacetylase that functions as a transcription repressor. *J. Biol. Chem.* **2000**, *275*, 15254–15264.
- Van den Wyngaert, I.; de Vries, W.; Kremer, A.; Neefs, J.-M.; Verhasselt, P.; Luyten, W. H. M. L.; Kass, S. U. Cloning and characterization of human histone deacetylase 8. *FEBS Lett.* **2000**, *478*, 77–83.
- Grozinger, C. M.; Hassig, C. A.; Schreiber, S. L. Three proteins define a class of human histone deacetylases related to yeast Hda1p. *Proc. Natl. Acad. Sci. U.S.A.* **1999**, *96*, 4868–4873.
- Kao, H.-Y.; Downes, M.; Ordentlich, P.; Evans, R. M. Isolation of a novel histone deacetylase reveals that class I and class II deacetylases promote SMRT-mediated repression. *Genes Dev.* **2000**, *14*, 55–66.
- Zhou, X.; Marks, P. A.; Rifkind, R. A.; Richon, V. M. Cloning and characterization of a histone deacetylase, HDAC9. *Proc. Natl. Acad. Sci. U.S.A.* **2001**, *98*, 10572–10577.
- Gao, L.; Cueto, M. A.; Asselbergs, F.; Atadja, P. Cloning and functional characterization of HDAC11, a novel member of the human histone deacetylase family. *J. Biol. Chem.* **2002**, *277*, 25748–25755.
- Finnin, M. S.; Donigian, J. R.; Cohen, A.; Richon, V. M.; Rifkind, R. A.; Marks, P. A.; Pavletich, N. P.; Breslow, R. Structures of a histone deacetylase homologue bound to the TSA and SAHA inhibitors. *Nature* **1999**, *401*, 188–193.
- Corminboeuf, C.; Hu, P.; Tuckerman, M. E.; Zhang, Y. Unexpected deacetylation mechanism suggested by a density functional theory QM/MM study of histone-deacetylase-like protein. *J. Am. Chem. Soc.* **2006**, *128*, 4530–4531.
- Lagger, G.; O'Carroll, D.; Rembold, M.; Khier, H.; Tischler, J.; Weitzner, G.; Schuettengruber, B.; Hauser, C.; Brunmeir, R.; Jenwein, T.; Seiser, C. Essential function of histone deacetylase 1 in proliferation control and CDK inhibitor repression. *EMBO J.* **2002**, *21*, 2672–2681.
- Zupkovitz, G.; Tischler, J.; Posch, M.; Sadzak, I.; Ramsauer, K.; Egger, G.; Grausenburger, R.; Schweifer, N.; Chiocca, S.; Decker, T.; Seiser, C. Negative and positive regulation of gene expression by mouse histone deacetylase 1. *Mol. Cell. Biol.* **2006**, *26*, 7913–7928.
- Glaser, K. B.; Li, J.; Staver, M. J.; Wei, R.-Q.; Albert, D. H.; Davidsen, S. K. Role of class I and class II histone deacetylases in carcinoma cells using siRNA. *Biochem. Biophys. Res. Commun.* **2003**, *310*, 529–536.
- Hoshikawa, Y.; Kwon, H. J.; Yoshida, M.; Horinouchi, S.; Beppu, T. Trichostatin A induces morphological changes and gelsolin expression by inhibiting histone deacetylase in human carcinoma cell lines. *Exp. Cell Res.* **1994**, *214*, 189–197.
- Bartl, S.; Taplick, J.; Lagger, G.; Khier, H.; Kuchler, K.; Seiser, C. Identification of mouse histone deacetylase 1 as a growth factor-inducible gene. *Mol. Cell. Biol.* **1997**, *17*, 5033–5043.
- You, A.; Tong, J. K.; Grozinger, C. M.; Schreiber, S. L. CoREST is an integral component of the CoREST-human histone deacetylase complex. *Proc. Natl. Acad. Sci. U.S.A.* **2001**, *98*, 1454–1458.
- Humphrey, G. W.; Wang, Y.; Russanova, V. R.; Hirai, T.; Qin, J.; Nakatani, Y.; Howard, B. H. Stable histone deacetylase complexes distinguished by the presence of SANT domain proteins CoREST/kiara0071 and Mta-L1. *J. Biol. Chem.* **2001**, *276*, 6817–6824.
- Hassig, C. A.; Fleischer, T. C.; Billin, A. N.; Schreiber, S. L.; Ayer, D. E. Histone deacetylase activity is required for full transcriptional repression by mSin3A. *Cell* **1997**, *89*, 341–347.
- Zhang, Y.; Iratni, R.; Erdjument-Bromage, H.; Tempst, P.; Reinberg, D. Histone deacetylases and SAP18, a novel polypeptide, are components of a human Sin3 complex. *Cell* **1997**, *89*, 357–364.
- Zhang, Y.; Sun, Z.-W.; Iratni, R.; Erdjument-Bromage, H.; Tempst, P.; Hampsey, M.; Reinberg, D. SAP30, a novel protein conserved between human and yeast, is a component of a histone deacetylase complex. *Mol. Cell* **1998**, *1*, 1021–1231.
- Alland, L.; David, G.; Shen-Li, H.; Potes, J.; Muhle, R.; Lee, H.-C.; Hou, H., Jr.; Chen, K.; DePinho, R. A. Identification of mammalian Sds3 as an integral component of the Sin3/histone deacetylase corepressor complex. *Mol. Cell. Biol.* **2002**, *22*, 2743–2750.
- Laherty, C. D.; Yang, W.-M.; Sun, J.-M.; Davie, J. R.; Seto, E.; Eisenman, R. N. Histone deacetylases associated with the mSin3 corepressor mediate Mad transcriptional repression. *Cell* **1997**, *89*, 349.

- (30) Tong, J. K.; Hassig, C. A.; Schnitzler, G. R.; Kingston, R. E.; Schreiber, S. L. Chromatin deacetylation by an ATP-dependent nucleosome remodelling complex. *Nature* **1998**, *395*, 917–921.
- (31) Xue, Y.; Wong, J.; Moreno, G. T.; Young, M. K.; Côté, J.; Wang, W. NURD, a novel complex with both ATP-dependent chromatin-remodeling and histone deacetylase activities. *Mol. Cell* **1998**, *2*, 851–861.
- (32) Zhang, Y.; Ng, H.-H.; Erdjument-Bromage, H.; Tempst, P.; Bird, A.; Reinberg, D. Analysis of the NuRD subunits reveals a histone deacetylase core complex and a connection with DNA methylation. *Genes Dev.* **1999**, *13*, 1924–1935.
- (33) Vannini, A.; Volpari, C.; Filocamo, G.; Casavola, E. C.; Brunetti, M.; Renzoni, D.; Chakravarty, P.; Paolini, C.; De Francesco, R.; Gallinari, P.; Steinkühler, C.; Di Marco, S. Crystal structure of a eukaryotic zinc-dependent histone deacetylase, human HDAC8, complexed with a hydroxamic acid inhibitor. *Proc. Natl. Acad. Sci. U.S.A.* **2004**, *101*, 15064–15069.
- (34) Karagiannis, T. C.; El-Osta, A. Will broad-spectrum histone deacetylase inhibitors be superseded by more specific compound? *Leukemia* **2006**, *21*, 61–65.
- (35) Bieliauskas, A.; Weerasinghe, S. V. W.; Pflum, M. K. H. Structural requirements of HDAC inhibitors: SAHA analogs functionalized adjacent to the hydroxamic acid. *Bioorg. Med. Chem. Lett.* **2007**, *17*, 2216–2219.
- (36) Beckers, T.; Burkhardt, C.; Wieland, H.; Gimmnich, P.; Ciossek, T.; Maier, T.; Sanders, K. Distinct pharmacological properties of second generation HDAC inhibitors with the benzamide or hydroxamate head group. *Int. J. Cancer* **2007**, *121*, 1138–1148.
- (37) Wang, D.-F.; Helquist, P.; Wiech, N. L.; Wiest, O. Toward selective histone deacetylase inhibitor design: homology modeling, docking studies, and molecular dynamics simulations of human class I histone deacetylases. *J. Med. Chem.* **2005**, *48*, 6936–6947.
- (38) Wang, D.-F.; Wiest, O.; Helquist, P.; Lan-Hargest, H.-Y.; Wiech, N. L. On the function of the 14 Å long internal cavity of histone deacetylase-like protein: implications for the design of histone deacetylase inhibitors. *J. Med. Chem.* **2004**, *47*, 3409–3417.
- (39) Estiu, G.; Greenberg, E.; Harrison, C. B.; Kwiatkowski, N. P.; Mazitschek, R.; Bradner, J. E.; Wiest, O. Structural origin of selectivity in class II-selective histone deacetylase inhibitors. *J. Med. Chem.* **2008**, *51*, 2898–2906.
- (40) Somoza, J. R.; Skene, R. J.; Katz, B. A.; Mol, C.; Ho, J. D.; Jennings, A. J.; Luong, C.; Arvai, A.; Buggy, J. J.; Chi, E.; Tang, J.; Sang, B.-C.; Verner, E.; Wynands, R.; Leahy, E. M.; Dougan, D. R.; Snell, G.; Navre, M.; Knuth, M. W.; Swanson, R. V.; McRee, D. E.; Tari, L. W. Structural snapshots of human HDAC8 provide insights into the class I histone deacetylases. *Structure* **2004**, *12*, 1325–1334.
- (41) Grozinger, C. M.; Schreiber, S. L. Deacetylase enzymes: biological functions and the use of small-molecule inhibitors. *Chem. Biol.* **2002**, *9*, 3–16.
- (42) Hassig, C. A.; Tong, J. K.; Fleischer, T. C.; Owa, T.; Grable, P. G.; Ayer, D. E.; Schreiber, S. L. A role for histone deacetylase activity in HDAC1-mediated transcriptional repression. *Proc. Natl. Acad. Sci. U.S.A.* **1998**, *95*, 3519–3524.
- (43) Pflum, M. K. H.; Tong, J. K.; Lane, W. S.; Schreiber, S. L. Histone deacetylase 1 phosphorylation promotes enzymatic activity and complex formation. *J. Biol. Chem.* **2001**, *276*, 47733–47741.
- (44) Hildmann, C.; Wegener, D.; Riestler, D.; Hempel, R.; Schober, A.; Merana, J.; Giurato, L.; Guccione, S.; Nielsen, T. K.; Figner, R.; Schwienhorst, A. Substrate and inhibitor specificity of class 1 and class 2 histone deacetylases. *J. Biotechnol.* **2006**, *124*, 258–270.
- (45) Riestler, D.; Hildmann, C.; Grünwald, S.; Beckers, T.; Schwienhorst, A. Factors affecting the substrate specificity of histone deacetylases. *Biochem. Biophys. Res. Commun.* **2007**, *357*, 439–445.
- (46) Li, J.; Staver, M. J.; Curtin, M. L.; Holms, J. H.; Frey, R. R.; Edalji, R.; Smith, R.; Michaelides, M. R.; Davidsen, S. K.; Glaser, K. B. Expression and functional characterization of recombinant human HDAC1 and HDAC3. *Life Sci.* **2004**, *74*, 2693–2705.
- (47) Schultz, B. E.; Misialek, S.; Wu, J.; Tang, J.; Conn, M. T.; Tahliramani, R.; Wong, L. Kinetics and comparative reactivity of human class I and class IIb histone deacetylases. *Biochemistry* **2004**, *43*, 11083–11091.
- (48) Cunningham, B. C.; Wells, J. A. High-resolution epitope mapping of hGH-receptor interactions by alanine-scanning mutagenesis. *Science* **1989**, *244*, 1081–1085.
- (49) Leung, H. B.; Schramm, V. L. A mutant AMP nucleosidase. Purification, properties, and in vivo turnover of the protein. *J. Biol. Chem.* **1981**, *256*, 12823–12829.
- (50) Parkin, D. W.; Mentch, F.; Banks, G. A.; Horenstein, B. A.; Schramm, V. L. Transition-state analysis of a V_{max} mutant of AMP nucleosidase by the application of heavy-atom kinetic isotope effects. *Biochemistry* **1991**, *30*, 4586–4594.
- (51) Liu, Y.; Shah, K.; Yang, F.; Witucki, L.; Shokat, K. M. A molecular gate which controls unnatural ATP analogue recognition by the tyrosine kinase v-Src. *Bioorg. Med. Chem.* **1998**, *6*, 1219–1226.
- (52) Northrop, J. P.; Ullman, K. S.; Crabtree, G. R. Characterization of the nuclear and cytoplasmic components of the lymphoid-specific nuclear factor of activated T cells (NF-AT) complex. *J. Biol. Chem.* **1993**, *268*, 2917–2923.
- (53) DeLano, W. L. The PyMOL Molecular Graphics System; Delano Scientific: San Carlos, CA, 2002.
- (54) Case, D. A.; Darden, T. A.; Cheatham, T. E., III; Simmerling, C. L.; Wang, J.; Duke, R. E.; Luo, R.; Merz, K. M.; Wang, B.; Pearlman, D. A.; Crowley, M.; Brozell, S.; Tsui, V.; Gohlke, H.; Mongan, J.; Hornak, V.; Cui, G.; Beroza, P.; Schafmeister, C.; Caldwell, J. W.; Ross, W. S.; Kollman, P. A. *AMBER 8*; University of California: San Francisco, 2004.
- (55) Stote, R. H.; Karplus, M. Zinc binding in proteins and solution: a simple but accurate nonbonded representation. *Proteins* **1995**, *23*, 12–31.
- (56) van Gunsteren, W. F.; Berendsen, H. J. C. Algorithms for macromolecular dynamics and constrained dynamics. *Mol. Phys.* **1977**, *34*, 1311.
- (57) Essman, U.; Perera, L.; Berkowitz, M. L.; Darden, T.; Lee, H.; Pedersen, L. G. Accuracy and efficiency of the particle mesh Ewald method. *J. Chem. Phys.* **1995**, *103*, 8557–8593.
- (58) Allen, M. P.; Tildesley, D. J. *Computer Simulation of Liquids*; Clarendon Press: Oxford, U.K., 1989.